Talanta 101 (2012) 32–37

Contents lists available at SciVerse ScienceDirect

Talanta

journal homepage: www.elsevier.com/locate/talanta

Folic acid as delivery vehicles: targeting folate conjugated fluorescent nanoparticles to tumors imaging

Jun Ai [a,b], Yuanhong Xu [a], Dan Li [a], Zuojia Liu [a], Erkang Wang [a,*]

[a] State Key Laboratory of Electroanalytical Chemistry, Changchun Institute of Applied Chemistry, Chinese Academy of Sciences, Changchun, Jilin 130022, China
[b] Graduate School of the Chinese Academy of Sciences, Beijing 100039, China

ARTICLE INFO

Article history:
Received 21 May 2012
Received in revised form
26 July 2012
Accepted 30 July 2012
Available online 12 September 2012

Keywords:
AuNPs
FITC
Folic acid
Bioimaging

ABSTRACT

Herein, folic acid (FA) conjugated with AuNPs were introduced into the cancer cell imaging via the specific interaction between FA and the folate receptor on the cell surface. FA protected gold nanoparticles (AuNPs) was synthesized and labeled with fluorescein isothiocynate (FITC) to form the FITC–FA–AuNPs (FFANPs). As over-expressed folic acid receptor in some cancer cells and folic acid can specifically and selectively combine, the FFANPs can bind to the FR expressed on tumor cells such as HeLa cells (human epithelial cervical cancer) and CERF-CEM cells (*T* cell line, human acute lymphoblastic leukemia). As a result, cancer cell imaging can be achieved. To ascertain the FR target ability, it has been acquired by FR-targeted images using synthetic FFANPs. The formation of FITC–FA can be identified by MS. FCM was carried out to study the cell uptake of FFANPs. The cell toxicity (3-[4,5–dimethylthiazolyl–2]−2, 5-diphenyltetrazolium bromide, MTT) assay demonstrated that the FITC-labeled conjugate had only little effect on the cytotoxicity to the cells, which further proved the applicability of the method in tumor cell imaging.

© 2012 Elsevier B.V. All rights reserved.

1. Introduction

With tremendous developments in nanotechnology over recent decades, great interest has arisen in using various nanomaterials for a wide range of bio-applications, such as bioanalysis, diagnosis, and biomedical treatment [1,2]. Among these nanomaterials, noble metal nanoparticles, especially gold nanoparticles (AuNPs), have displayed particular prospects to achieve these tasks, due to their unique chemical/physical properties, and other advantages such as simple synthesis, good biocompatibility, and easy conjugation with biomolecules [1–3]. For example, in the past decade, AuNPs have been used as soluble gold for esthetic and medical purposes [4]. Nuclear targeting of AuNPs in cancer cells resulted in DNA damage, cytokinesis arrest, and ultimately cell death [5]. They were also proven to preferentially accumulate at sites of tumor growth/inflammation and enter cells by mechanisms very different from and much more rapid than those of small molecules [6]. Recently, to realize real "green chemistry" that requires low toxicity but high activity, directly importing biological and biomimetic molecules into AuNPs synthesis started to attract increasing attention and was considered to be a desirable choice to develop non-invasive strategies for future diagnosis, imaging, and cancer treatment [6]. Even though some progresses have been made, it is still a promising field that expects much more effort and exploration.

Folic acid (FA), also known as folacin and folate, was a high affinity binding reagent that could recognize folate receptor (FR), which was a tumor marker over-expressed on the surface of many human tumor cells, including ovarian, lung, breast, kidney, endometrial, and renal [7–12]. It was found that when FA was chemically linked with c-carboxyl groups, its FR binding affinity was hardly affected. Therefore, it has been studied widely as a recognition element for imaging and cancer therapy over the last two decades, with ability to conjugate with anti-cancer drugs or nanomaterials for tumor targeting [13].

In this study, we used FA as protecting reagent to synthesize AuNPs, followed by conjugating the FA–AuNPs with FITC to form FITC–FA-protected Au NPs (FAANPs). MALDI-TOF MS was employed to confirm the structure of the FITC–FA complex. A laser scanning confocal microscope (LSCM) was used to characterize the intracellular uptake of FAANPs. Furthermore, the cytotoxicity of FAANPs was investigated by 3-[4,5–dimethylthiazol–2–yl]−2,5-diphenyl tetrazolium bromide (MTT) assay, and a transfection assay by FAANPs. At last, by using FA as FR recognizer and FITC as fluorescent reporter, we proved that such FAANPs could serve very well as a probe-reporter dual-function reagent in realizing cell imaging and cell transfection by HeLa cells (FR overexpression) (Fig. 1). Recently, Fadeel et al. has illustrated that nanoparticles functioned with FA can be utilized for targeting and imagining cancer cells which

* Corresponding author: Tel.: +86 431 85262003; fax: +86 431 85689711.
E-mail address: ekwang@ciac.jl.cn (E. Wang).

0039-9140/$ - see front matter © 2012 Elsevier B.V. All rights reserved.
http://dx.doi.org/10.1016/j.talanta.2012.07.075

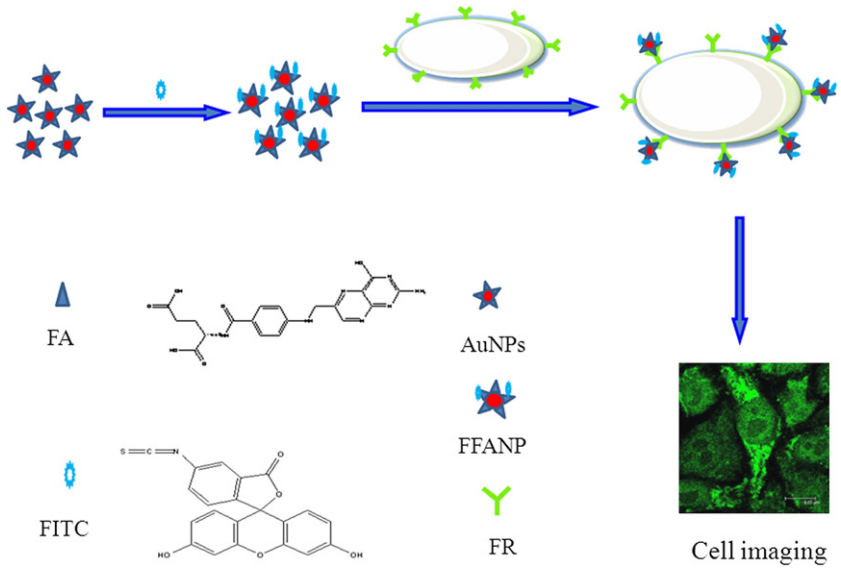

Fig. 1. Principle of FFANPs bioimaginged in HeLa cells and CCRF-CEM cells: first step, FA protected AuNPs was synthesized and the nanoparticles was lablled with FITC; second step, HeLa cells and CCRF-CEM cells were fed with FFANPs and then FR specially connected with FA. Thus, the FFANPs inserted cells and completed bioimaging.

overexpress FR, however, covalent modification of nanoparticle with FA was required [14]. Herein, to eliminate the trivial procedures and improve the transfection efficiency, we synthesized gold nanoparticles using FA as protecting reagent and simplified the method of FA functionalization of nanoparticles. Moreover, it was demonstrated that the FA protected gold nanoparticles can target cancer cells very well through LSCM and FCM characterization.

2. Materials and methods

2.1. Chemicals and materials

Chloroauric acid ($HAuCl_4$) was purchased from Aldrich (USA). FA was purchased from Sigma (USA). Sodium hydroxide (NaOH) and all chemicals of analytical grade were used as received without further purification. 3-[4,5–dimethylthiazolyl–2]−2, 5-diphenyltetrazolium bromide were obtained from Sigma–Aldrich (USA). Phosphate buffered solution (PBS) [10 mM phosphate (NaH_2PO_4 and Na_2HPO_4), pH=7.4] was also prepared. The PBS buffer was used to rinsing suspension of HeLa cells. All the solutions were prepared by using distilled water and stored at 4 °C before use. HeLa cells were obtained from the American Type Culture Collection (Manassas, VA) and maintained in DMEM supplemented with 10% standard Fetal bovine serum (Defined FBS) (HyClone Laboratories, UT) at 37 °C and in 5% CO_2. Glass chamber slides (14 mm bottom well) were purchased from Hangzhou Sanyou Biotechnology Co. Ltd. (Hangzhou, China).

2.2. Apparatus

UV/Vis absorption spectra were carried out by a CARY 500 UV/Vis/near-IR spectrophotometer (Varian). Fluorescence measurements were recorded at room temperature using a LS 55 luminescence spectrometer (Perkin–Elmer). The sample for cell imaging was obtained by fixing the bound cells using FAANP on a 35-mm tissue culture dish (World Precision Instruments) and the result of fluorescence images were acquired using LEICA TCS SP2 laser scanning confocal microscope (Germany) with a 100 × oil immersion objective. TEM images were obtained with a FEI TECNAI G^2 transmission electron microscope (Netherlands) operating at a voltage of 120 kV. The samples for TEM characterization were prepared by placing a drop of colloidal solution on carbon-coated copper grid and dried at room temperature. The result of MTT was obtained from EL808 ultramicroplate reader (Bio-TEK Instrument, Inc., Winooski, VT, USA).

2.3. Synthesis of FA-protected AuNPs and connected with FITC

Synthesis of FA-protected AuNPs was referenced to literature [15]. The experimental process was as follows: FA has a poor solubility in water. So, it was dissolved by adding NaOH. In short, 0.012 g FA powder was mixed with 10 mL H_2O, and then approximately 100 μL 1.0 M NaOH solution was added to the above turbid solution until it came to clear. During a typical synthesis, the prepared FA solution was added drop by drop to the 0.972 mM $HAuCl_4$ 5 mL solution under magnetic stirring, and the light yellow $HAuCl_4$ solution turned slightly darker and some precipitate emerged. The precipitate was regarded as FA, which was insoluble at lower pH when encountering $HAuCl_4$. For this reason, a further amount of 180 μL 0.1 M NaOH was subsequently added to obtain a clear solution with a bright orange color. Half an hour later, the system was heated to 50 °C and the reaction continued for 6 h until a transparent red solution was obtained. The as-prepared FA–Au NPs solution was centrifuged at 10000 rpm for 10 min to remove the free FA and then washed three times for subsequent measurements. At room temperature, FFANPs was obtained by FITC mixing with FA–Au NPs.

2.4. Bioimaging

HeLa cells and CCRF-CEM cells incubated with FFANPs. HeLa cells and CCRF-CEM cells were plated onto 35 mm glass chamber slides. Stock solutions of FFANPs in PBS buffer were prepared at concentrations of 10 μM. Diluted solutions in complete growth medium were then freshly prepared and placed over the cells for 2–3 h. All cells were washed with PBS buffer (3 ×) at room temperature. After that, cells were scanned by LEICA TCS SP2 laser scanning confocal microscope (LSCM). HeLa cells (10^6 cells per sample) were washed three times with PBS buffer (pH=7.4). Then 100 μM FFANPs was added to the treated cells in PBS (pH 7.4), and further incubated for 2 h at 37 °C. The fluorescent signal in living cells could be monitored qualitatively; However, FCM might be applied to detect the binding affinity quantitatively. Thereafter, cells were analyzed by flow cytometric

analysis. A total of 10,000 events were acquired for each sample. Background binding in the presence of PBS alone was 1.0% for HeLa cells. The cells were washed twice with PBS (pH=7.4) and coincubated in the presence of 5 μM FFANPs for 2 h at 37 °C.

2.5. Flow cytometric analysis

The samples were analyzed by a FACSAria analyzer (Becton Dickinson Immunochemical Systems, Mountain View, CA). A typical cell area was gated and more than 10,000 events were counted. An isotype negative control was used to define the threshold of the background staining. The result was expressed in percentage of the gated cells. The negative control was always less than 5%. Thus, the result of the sample that was more than 5% was considered as positive. For the HeLa cell lines, the flow cytometric analysis was done in triplicates.

2.6. MTT assay

In order to evaluate the FFANPs dose on cellular toxicity, the complex treated cells were illuminated for a serial concentration. After treatment, cells were incubated in fresh medium for 24 h. The culture medium was replaced by 100 μL fresh medium containing 0.5 mg/mL 3-[4,5–dimethylthiazol–2–yl]− 2,5-diphenyl tetrazolium bromide assays reagent, and then incubated at 37 °C and 5% CO_2 for 4 h. Then, the MTT containing medium was added with 100 μL of acid/isopropanol solution, in which the concentration of HCl was 0.04 M to dissolve the MTT product, formazan. Viability of non-silver nanocluster-treated control cells was arbitrarily defined as 100%. Finally, the absorption at 490 nm of each well was measured by a EL808 ultramicroplate reader. The relative cell viability was recorded and shown (Fig. 6).

3. Results and discussion

3.1. The bioimaging design of FFANPs

In this work, FA protected AuNPs were synthesized and labeled with FITC to form the FITC–FA–AuNPs (FFANPs). By using FFANPs as the bioimaging element, we reported a simple and sensitive FITC-based FFANPs method for cancer detection in PBS system. The designed bioimaging strategy by using FFANPs as the recognition and fluorescence element was shown in Fig. 1. The synthesis route for the fluorescence complex FFANPs and bioimaging process were demonstrated as follows. First, a facile method to obtain FA-protected Au NPs by heating an aqueous solution of $HAuCl_4$/FA in which FA acts as both the reducing and stabilizing agent. Second, FITC covalently labeled onto FA-protected AuNPs and FFANPs was formed in PBS buffer and finally, FFANPs were connected by FR in HeLa cells and CCRF-CEM cells and then resulted in bioimaging. The bioimaging principle was based on FA specially binding of FR in the cell.

3.2. MS detection and fluoresence detection of FFANPs

It was reported that isothiocyano group of FITC could react with amino group of FA to form the thiourea [16]. In order to validate FITC could be connected with FA, the solution was

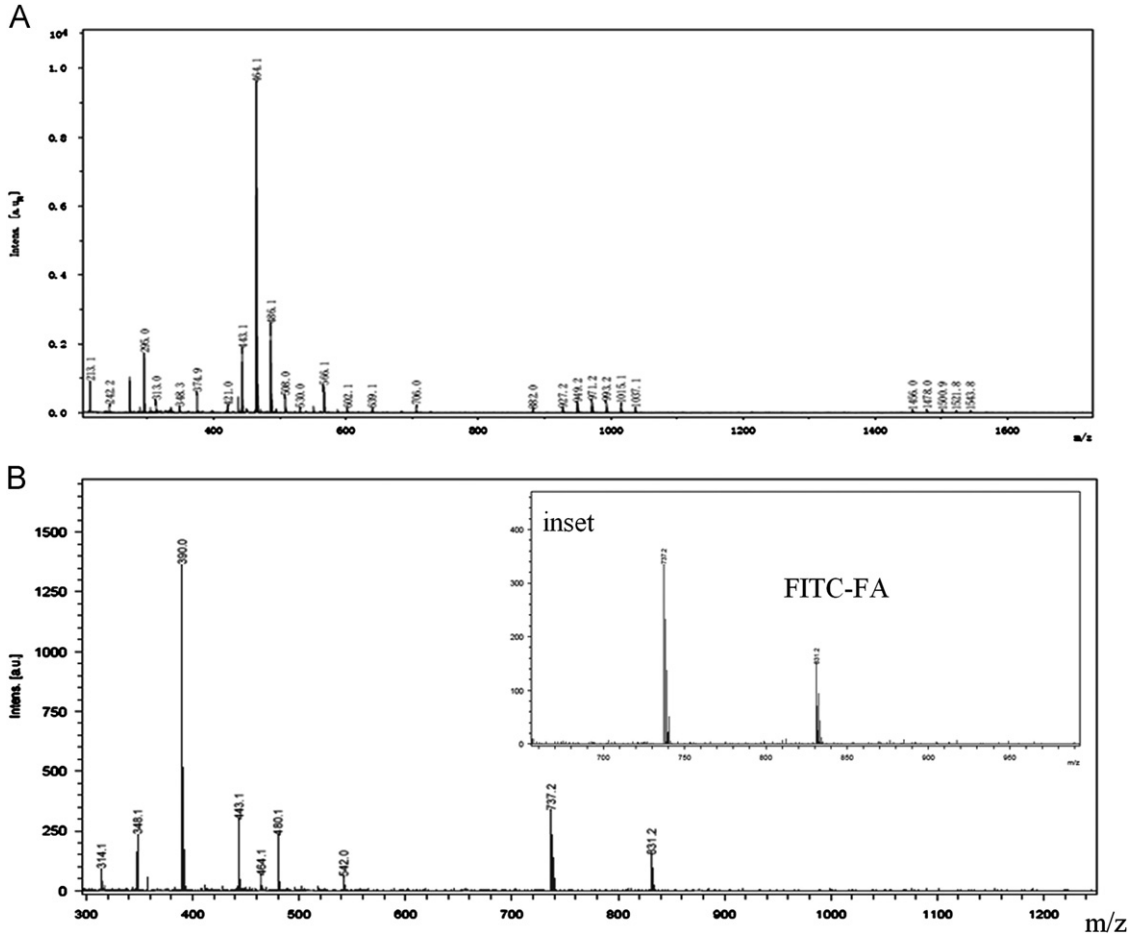

Fig. 2. MALDI-TOF mass spectra of FA (A) and FITC–FA (B). Inset was magnifying spectrum of *b* in scale 700–1000(m/z).

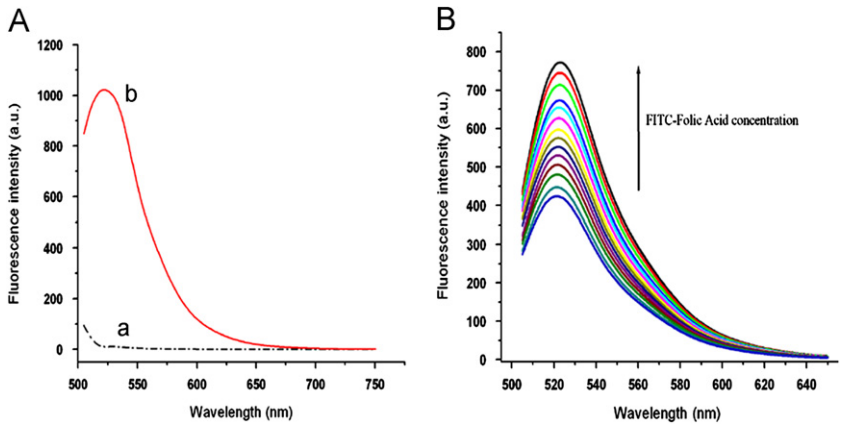

Fig. 3. Fluorescence spectra of (A) 10 μM FA (a) and 10 μM FFANPs (b); and fluorescence spectra of (B) FITC with increasing FFANPs concentrations of 0.05, 0.1, 0.2, 0.4, 0.8, 1.0, 1.5, 2.0, 2.5, 3.0, 4.0, 5.0 and 6.0 μM, respectively. Background buffer: 50 mM PBS buffer (pH=7.4); excitation length: 488 nm.

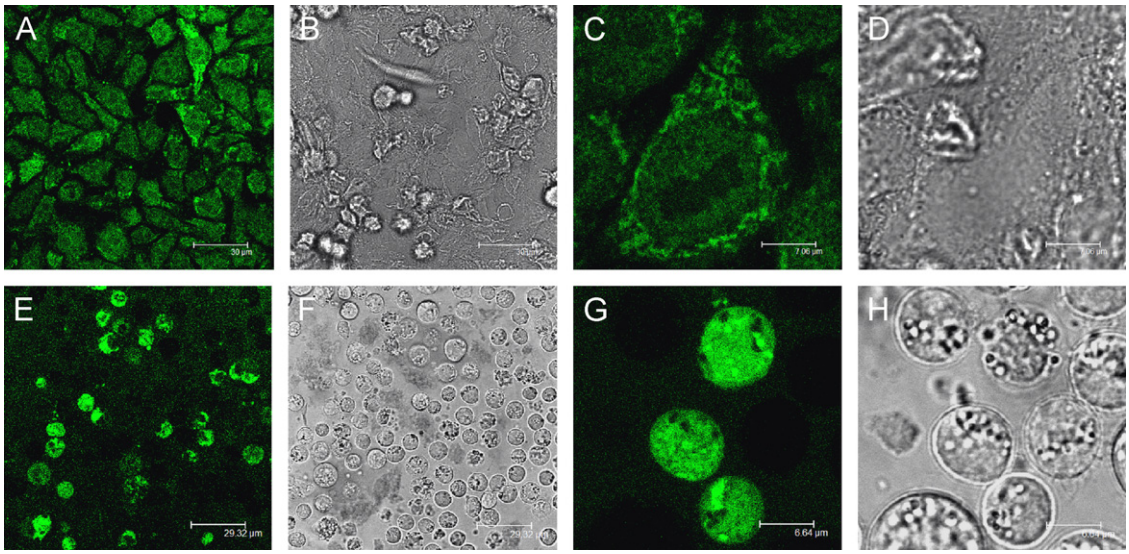

Fig. 4. B,D: bright-field image and A,C: fluorescence image of live hela cells incubated with FFANPs for 2 h at 37 °C ([FFANPs]=15 nM); F,H: bright-field image and E,G: fluorescence image of live CCRF-CEM cancer cells after incubation with FFANPs for 2 h at 37 °C ([FFANPs]=100 nM).

investigated by MALDI-TOF MS. The molecular weight of FITC and FA was 389.38 and 441.40, respectively. As shown in Fig. 2. m/z of 831 had a peak, it was indicated that FITC could be connected with FA. The fluoresence detection was based on FA-protected AuNPs. It can be seen from Fig. S1 that an absorption band at 532 nm appears in the final fluorescent AuNPs solutions. The size and shape of the AuNPs were examined with selected FA/$HAuCl_4$ ratios (0.56:1) [4] using transmission electron microscopy (TEM). The morphologies of AuNPs were studied by high-resolution transmission electron microscopy (HR-TEM), which were shown in Fig. S2. (ESI). The results reveal that the spherical AuNPs can be clearly distinguished due to the high electron density of the molecule. Fig. S3. illustrated the TEM spectrum of FA conjugated AuNPs (A) and FFANPs (B) with HeLa cells (human epithelial cervical cancer) and TEM images of FA conjugated AuNPs (C) and FFANPs (D) with CERF-CEM cells. The result indicated that TEM spectrum of FFANPs with cancer cells compared with FA conjugated AuNPs were well dispersed. Fig. 3. (A) indicated that the fluorescence emission spectra of FFANPs and FA at 488 nm excitation. From the figure, we can conclude that when FFANPs and FA have same concentration, the fluorescence emission intensity of FFANPs was strong while the fluorescence intensity of FA was very weak at 488 nm excitation. FA at 10 μM concentration in PBS solution showed a very weak fluorescence at 522 nm emission. However, the fluorescence signal was introduced by FITC in the complex of FITC and FA at 522 nm. It was clearly demonstrated that FA had no contribution to fluorescence signal of FFANPs. In order to confirm the relationship between concentration and fluorescence signal, different concentrations of FFANPs were detected by the LS 55 luminescence spectrometer. The result of Fig. 3(B) demonstrated that when excitations at 488 nm resulted in an emission at 522 nm, the fluorescence intensity of FFANPs was enhanced with increasing concentration.

3.3. Cell imaging of FFANPs

Owing to its favorable spectroscopic properties of the response to FR, FFANPs should be suited for fluorescence imaging in living tumor cells. HeLa cells and CCRF-CEM cells were stained with a 100 nM solution of FFANPs in PBS buffer for 30 min at 37 °C and 5% CO_2, followed by determination using laser scanning confocal microscope. A significant increase of fluorescence from the intracellular area was observed (Fig. 4). It was visibly shown that the localization of culture dish labeled with the bioconjugate. HeLa cells were adherent cells and CCRF-CEM cells were suspension cells. Having confirmed the cellular uptake of the fluorescent complex, the FFANPs were investigated by cell imaging compared with different tumor cells, known for its

efficiency in culture dish staining. The images were acquired via confocal microscopy and shown in Fig. 4, panels A–H. Imaging results with the FFANPs were reproducible in HeLa cells and in accordance with images using the CCRF-CEM. FA was taken up by the FR on the cell membrane and it acted as a predecessor of tetrahydrofolate in the nucleus [17]. This phenomena demonstrated that the FFANPs could combine with FR of HeLa cells and CCRF-CEM cells. Thus, these results explained that FFANPs could be used for nanomaterial of detecting cancer cells [15].

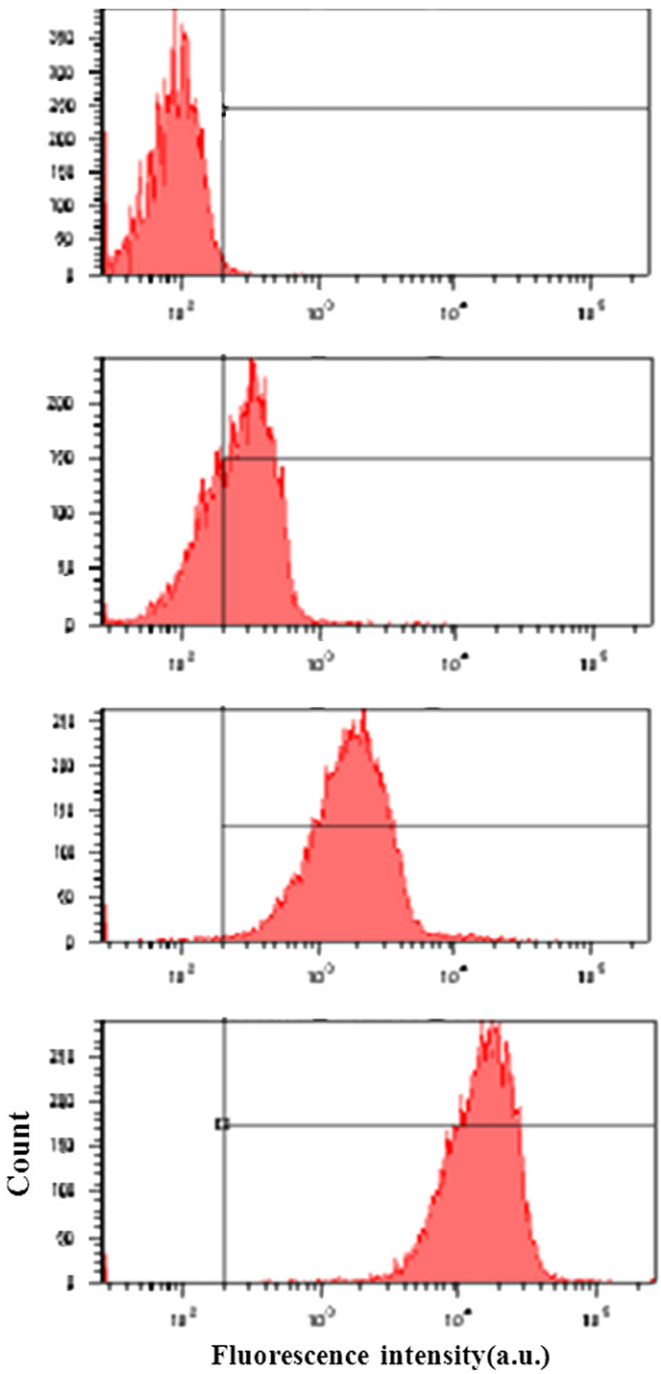

Fig. 5. A typical flow cytometric histogram of binding FFANPs to HeLa cells. The cells were incubated with FFANPs (0, 1.5 nM, 15 nM and 150 nM) in PBS buffer for 2 h at 37 °C and then analyzed by FCM. One representative experiment of the three performed is shown. FFANPs exhibited a strong positive staining by FA, whereas the corresponding HeLa cells in the absence of FFANPs showed negative.

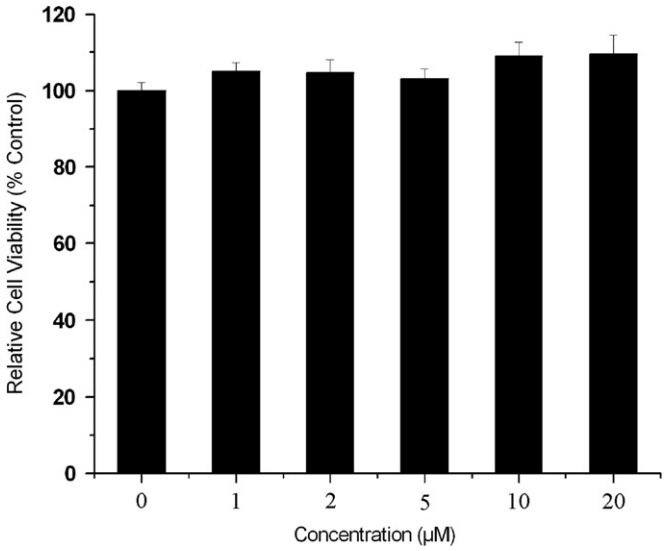

Fig. 6. Cytotoxicity of the FFANPs on HeLa cells was measured by MTT assays ($n=8$, mean $\pm$S.D.). The result showed the relative cell viability of the cells accompanied with FFANPs with the final concentrations of 0, 1, 2, 5, 10 and 20 μM. The viability of positive control that treated with same volume of water was taken as 100%.

3.4. FCM assay of FFANPs

After understanding the fluorescence characteristics, binding modes and bioimaging of the FFANPs complex, the intracellular uptake of the FFANPs complex was estimated from the fluorescence intensities of HeLa cells by a flow cytometry (Fig. 5). We have confirmed a better insight into the interaction between FFANPs and FR of cells. To further assess the binding specificity and fluoresence signal, we measured the binding of FFANPs to HeLa cell line. Through this approach, the sensitive detection of average FR expressed at the surface of 10,000 HeLa cells was accomplished by FCM. It could be seen clearly in Fig. 5. That was a positive fluorescence shift appeared with the increasing of FFANPs concentration. The results of FFANPs–transformed HeLa cells expressing FR suggested the formation of the FFANPs–FR complexes. It indicated that the flow cytometric data and fluorescence images depended on the degree of the FR expression by using FFANPs.

3.5. MTT assay of the size of FFANPs

The cytotoxicity of the FFANPs on the cell proliferation used in our system was investigated by MTT assay. Fig. 6. showed the data of cell viability of the HeLa cells after 24 h of incubation with the transfection complexes. Non-transfected cells were severed as the control and the cell viability of which was set as 100%. It was found that the FFANPs for the transfection had hardly any toxicity to the cells. In the presence of FFANPs, the cell viabilities increased to be more than 80% for both of the transfection systems. With addition of FFANPs at the concentration of 20 μM, the cell viabilities for FFANPs did not decrease. These results indicated that FFANPs exhibited no apparent cytotoxicity to HeLa cells and were favorably biocompatible.

4. Conclusion

FA-protected Au NPs was synthesized by heating an aqueous solution of $HAuCl_4$/FA in which FA acts as both the reducing and stabilizing agent. The AuNPs was labeled with FITC to form FFANPs. FFANPs were introduced to the bioimaging of biomarker FA through

specific interaction of cell surface FR in living HeLa cells and CCRF-CEM cells. The phenomenon of cell imaging was characterized by LSCM. Meanwhile, MALDI-TOF MS confirmed that FA was labeled with FITC by forming thiourea. According to the results of FCM, the cell uptake of FFANPs was further verified. The cell toxicity MTT assay demonstrated that the FITC-labeled conjugate had only little effect on the cytotoxicity to the cells. These results indicated the developed method for FFANPs imaging was simple and cost-effective. It was predicted that exploiting new functions of existing nanomaterial would extend their applications in bioanalysis.

Acknowledgments

This work was supported by the National Natural Science Foundation of China, Grant nos. 21075120, 21190040, and 973 projects 2009CB930100 and 2011CB911000.

Appendix A. Supporting information

Supplementary data associated with this article can be found in the online version at http://dx.doi.org/10.1016/j.talanta.2012.07.075.

References

[1] X. Huang, I.H. El-Sayed, W. Qian, M.A. El-Sayed, Nanomedicine 2 (2007) 681–693.
[2] J.A. Barreto, W. O'Malley, M. Kubeil, B. Graham, H. Stephan, L. Spiccia, Adv. Mater 23 (2011) H18–H40.
[3] A.D. Tiwari, A.K. Mishra, S.B. Mishra, O.A. Arotiba, B.B. Mamba, Int J. Biol. Macromol. 48 (2011) 682–687.
[4] G. Li, D. Li, L. Zhang, J. Zhai, E. Wang, Chem. Eur J. 15 (2009) 9868–9873.
[5] B. Kang, M.A. Mackey, M.A. El-Sayed, J. Am. Chem. Soc. 132 (2010) 1517–1519.
[6] E.C. Dreaden, A.M. Alkilany, X. Huang, C.J. Murphy, M.A. El-Sayed, Chem. Soc. Rev. 41 (2012) 2740–2779.
[7] J. Hou, Q. Zhang, X. Li, Y. Tang, M.R. Cao, F. Bai, Q. Shi, C. Yang, D. Kong, G. Bai, J. Biomed. Mater. Res. A 99A (2011) 684–689.
[8] S. Santra, C. Kaittanis, O.J. Santiesteban, J.M. Perez, J. Am. Chem. Soc. 133 (2011) 16680–16688.
[9] I.G. Campbell, T.A. Jones, W.D. Foulkes, J. Trowsdale, Cancer Res. 51 (1991) 5329–5338.
[10] S.D. Weitman, A.G. Weinberg, L.R. Coney, V.R. Zurawski, D.S. Jennings, B.A. Kamen, Cancer Res. 52 (1992) 6708–6711.
[11] S.D. Weitman, R.H. Lark, L.R. Coney, D.W. Fort, V. Frasca, V.R. Zurawski, B.A. Kamen, Cancer Res. 52 (1992) 3396–3401.
[12] M.J. Mattes, P.P. Major, D.M. Goldenberg, A.S. Dion, R.V.P. Hutter, K.M. Klein, Cancer Res. 50 (1990) 880–884.
[13] S.L. Kim, H.J. Jeong, E.M. Kim, C.M. Lee, T.H. Kwon, M.H. Sohn, J. Korean Med. Sci. 22 (2007) 405–411.
[14] A. Garcia-Bennett, M. Nees, B. Fadeel, Biochem. Pharmacol. 81 (2011) 976–984.
[15] A.N. Shipway, I. Willner, Chem. Phys. Chem. 1 (2000) 18–52.
[16] H. Maeda, N. Ishida, H. Kawauchi, K. Tuzimura, J. Biochem. 5 (1969) 777–783.
[17] J.Y. Wong, T.L. Kuhl, J.N. Israelachvili, N. Mullah, S. Zalipsky, Science 275 (1997) 820–822.